

Numerical study on H₂ / Air Flame Jet Ignition to Clarify the Behavior of Flame Propagation

Hajime BITOH, Makoto ASAHARA, Eisuke YAMADA, A. Koichi HAYASHI
Dept. of Mech. Eng., Aoyama Gakuin Univ
5-10-1, Fuchinobe, Chuo, Sagamihara, Kanagawa, 252-5258, Japan

1. Introduction

A lot of attentions have been paid to hydrogen as a fuel of next generation today. Hydrogen produces only water from its combustion unlike hydrocarbons. However its burning rate is so fast that it may cause explosion easily. Two years ago we had Fukushima Daiichi Nuclear Power Plant accident after the big earthquake, which might be triggered by a jet ignition of hydrogen. Jet ignition can be referred probably its first application by Gussak in 1976^[1] and 1983^[2], who developed the jet ignition engine named by LAG (Avalanche Activated Combustion). By this method we can burn a quite lean mixture of fuel where a conventional spark igniter cannot ignite. Oppenheim et al. studied and developed jet igniter to apply a real engine since 1980s^[3] and 1990s^[4]. He used plasma jet igniter (PJI) and flame jet igniter (FJI) and compared them for their energy efficiency. One of a good example of FJI igniter application to engine can be found in a work done by Hensinger et al.^[5] And Hyashi et al.^[6] Suetake et al.^[7] studied a fundamental of jet ignition experimentally and numerically in 1999. They used a chamber which has two rooms divided by a wall with a hole at its center. The map of ignition mode at receiver chamber in hydrogen/air mixture is shown in Fig. 1 concerning to orifice size and equivalence ratio. They could map ignition for three types; jet ignition, transient ignition, and auto ignition. Auto ignition in their case implies that the ignition occurs at the receiver chamber just before the flame goes through the hole of the separated wall. The experimental chamber configuration is shown in Fig. 1. Later Asami et al.^[8] measured OH profiles of jet ignition using LIF measurement system to see the development and propagation mechanism of jet ignition. At the almost same time Jordan et al. studied jet ignition in a similar configuration of combustion chamber, but they did not get so-called auto-ignition. The present study will show the detailed mechanism of flame jet ignition numerically using a detailed chemical reaction mechanism of hydrogen together with some of Suetake's experimental results.

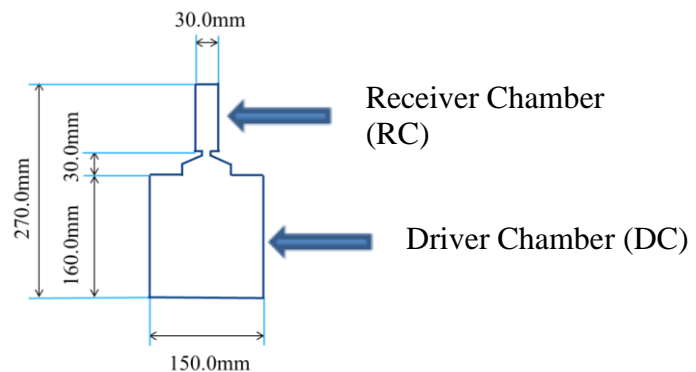


Figure 1 Configuration of combustion chamber for FJI system

2. Mechanism of FJI

This action is an explanation about the detailed mechanism of FJI. FJI has three types of ignition Suetake et al.^[7]. Fig.2 shows a map of ignition related to the orifice size and equivalence ratio. The first, a flame type is a typical Jet Ignition indicated by the circle symbol in Fig.2 where the flame is ignited by a spark plug in DC, the flame passing through the orifice, and propagating in RC with a high flame speed. The second type ignition is similar as Auto Ignition. A flame is ignited in RC before flame pass through the orifice. Final type is transient ignition that Jet Ignition and Auto Ignition are exist at the same time. This type can not be distinguished whether Jet Ignition or Auto-Ignition. All ignition types have a high thermal efficiency. However, it is not clear what classifies three types of ignition. Asami et al.^[3] studied FJI using a LIF measurement with the same experimental container as Suetake. It is suggested that compression wave and the shape of container affect on FJI phenomena.

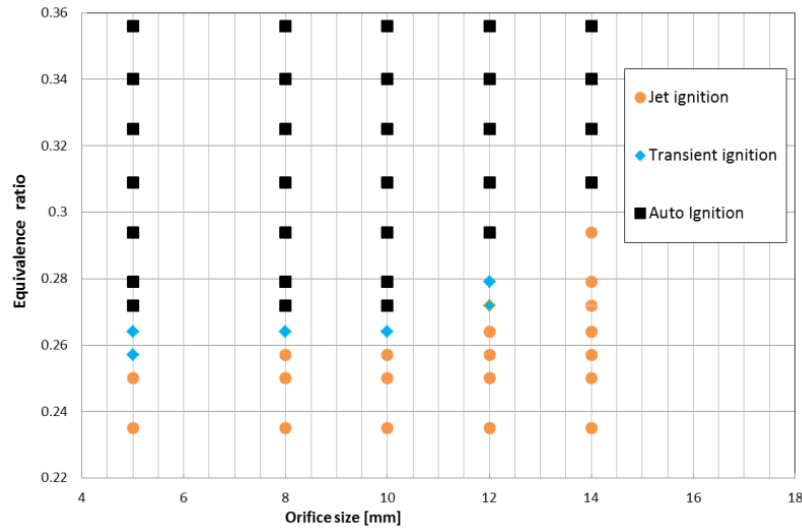


Figure 2 Combustion mode of jet ignition

3. Formulation and numerical method

We calculate FJI in the 2 dimensional region with CFD++^[9]. The chemically reacting fluid was described by Navier – Stokes equations. The Navier – Stokes equations are integrated by using TVD scheme for the convective terms and Large Eddy Simulation model for turbulent model. The equation of continuity and momentam and energy equations is

$$\frac{\partial Q}{\partial t} + \frac{\partial}{\partial x}(F_1 + G_1) + \frac{\partial}{\partial y}(F_2 + G_2) = \dot{S} \cdot \cdot \cdot (1)$$

$$Q = \begin{bmatrix} e \\ \rho \\ \rho u \\ \rho v \end{bmatrix}, F_1 = \begin{bmatrix} (e+p)u \\ \rho u \\ \rho u^2 + p \\ \rho v u \end{bmatrix}, F_2 = \begin{bmatrix} (e+p)v \\ \rho v \\ p u v \\ \rho u^2 + p \end{bmatrix}, G_1 = \begin{bmatrix} \dot{q}_x - u\tau_{xx} - v\tau_{xy} \\ 0 \\ -\tau_{xx} \\ -\tau_{xy} \end{bmatrix}, G_2 = \begin{bmatrix} \dot{q}_y - u\tau_{yx} - v\tau_{yy} \\ 0 \\ -\tau_{yx} \\ -\tau_{yy} \end{bmatrix}$$

$$\tau_{xx} = 2\mu \frac{\partial u}{\partial x} - \frac{2}{3}\mu\Phi$$

$$\tau_{yy} = 2\mu \frac{\partial v}{\partial y} - \frac{2}{3}\mu\Phi$$

$$\tau_{xy} = \tau_{yx} = \mu \left(\frac{\partial u}{\partial y} + \frac{\partial v}{\partial x} \right)$$

The Smagorinsky sub - grid scale stress model has been incorporated in the above equations so that $\mu_{eff} = \mu + \mu_T$ with μ_T being the turbulent viscosity given by the Smagorinsky – Lilly model as

$$\rho \overline{u v} = \rho \overline{u v} + 2\mu_T \overline{s}_{ij} + \frac{1}{3} R_{kk} \delta_{ij}$$

$$\mu_T = \rho (C_S \Delta)^2 |\overline{s}| = \rho (C_S \Delta)^2 (2\overline{s}_{ij} \overline{s}_{ij})^{1/2}, \overline{s}_{ij} = \frac{1}{2} \left(\frac{\partial u}{\partial y} + \frac{\partial v}{\partial x} \right) \cdot \cdot \cdot (2)$$

where C_S is the sub – grid scale stress constant and $\Delta = (\Delta x \Delta y)^{1/2}$ defined by the grid spacing. Bouris and Bergeles^[10] insist that the two – dimensional large eddy simulation using a fine grid resolution gives a better representation than using RANS model and more complex models offer only a slight improvement at the expense of computational time. The ignition region is 2cm×2cm square which the center of the ignition area height is located 1.5cm, lateral is located in the center. Figure 3 shows the ignition region and the location of pressure gage. To model chemical reactions, we use a detailed chemical reaction model^[11] which consists of 9 species and 18 elementary reactions. The size of the computational domain is the same as that used by Suetake et al.^[2]. The grid sizes are 0.2mm square. Table 1 shows the initial condition of this study. Presently we are calculating smaller grid, 10 μ m square.

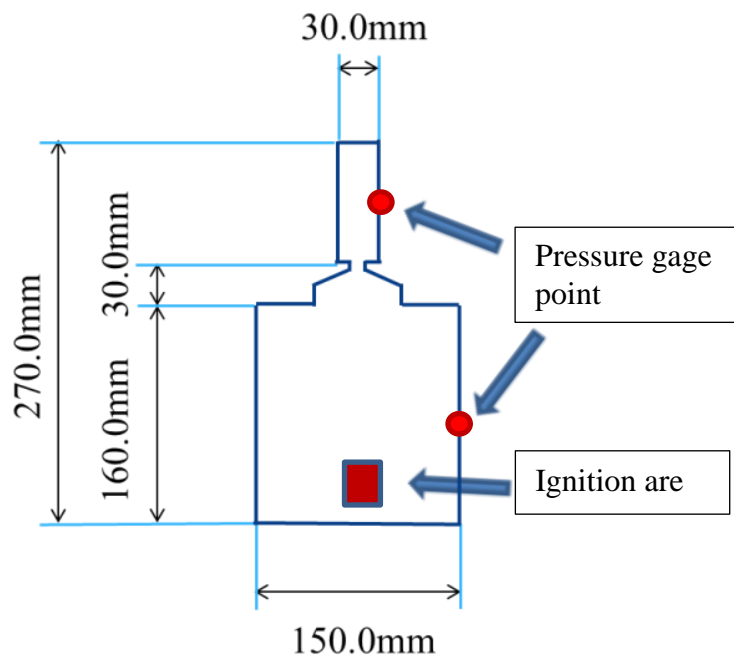


Figure 3 Pressure gage point and Ignition location at the present calculation

Table 1 Initial condition

Orifice size [mm]	5.0	14.0
Initial Pressure [Mpa]	0.10	0.10
Initial Temperature [K]	293	293
Equivalent ratio	0.340	0.340

4. Result and discussion

Figure 4 shows the pressure comparison between experiment and calculation in case of 5mm diameter of orifice. Each start time is when flame enters the MC. It is confirmed that the maximum pressure is different from experiment and calculation, but the graph shape is almost consistent.

Figures 5 – 8 show the time history of the density distribution and the temperature distribution in the Receiver Chamber of the combustor at 5ms times interval. The orifice diameter is 5mm in Figs.5 and 7, 14mm in Figs.6 and 8. Jet ignition has been confirmed in 5mm case shown in Figs.5 and 7, which is not confirmed in 14mm. The flame in 14mm does not propagate in RC seen in Figs.6 and 8. It is clarified that the flame shape before passing through the orifice is changed by changing the orifice diameter. This difference of flame shape before passing through the orifice affects the type of the flame propagation after passing. It is considered that the way of reflection dynamics of the compression wave which occur at the first ignition depends on the orifice diameter.

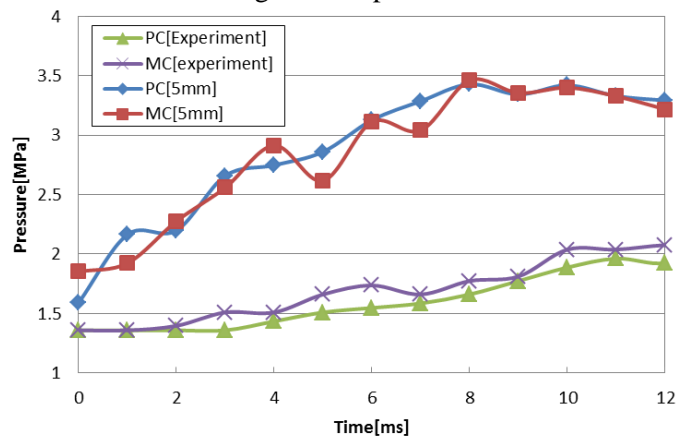


Figure 4 Pressure comparison

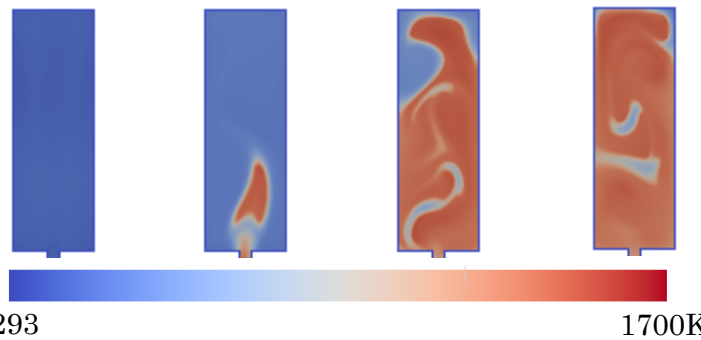


Figure 5 Time history of temperature distribution in case of 5mm orifice diameter

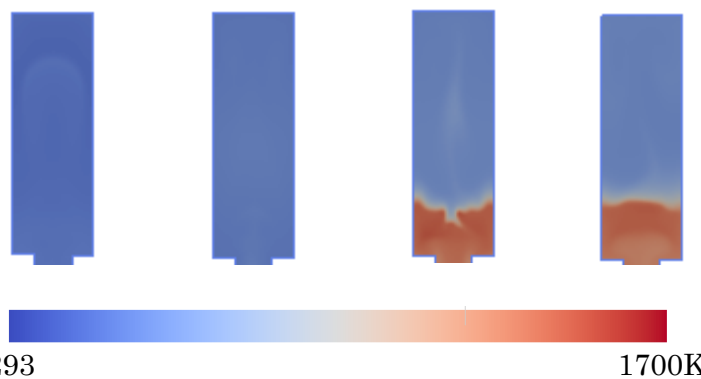


Figure 6 Time history of Temperature in case of 14mm orifice diameter

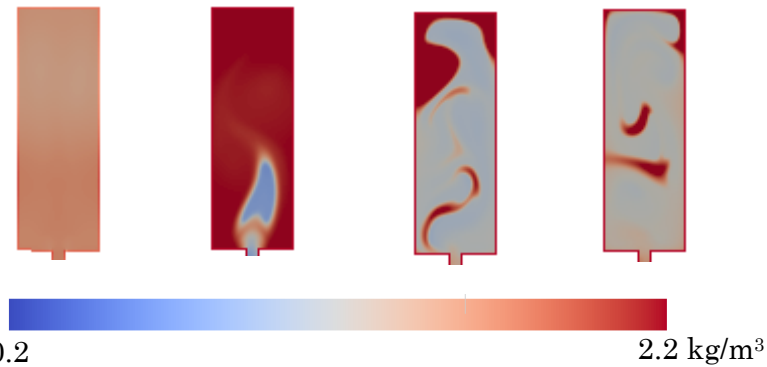


Figure 7 Time history of density distribution in case of 5mm diameter of orifice.

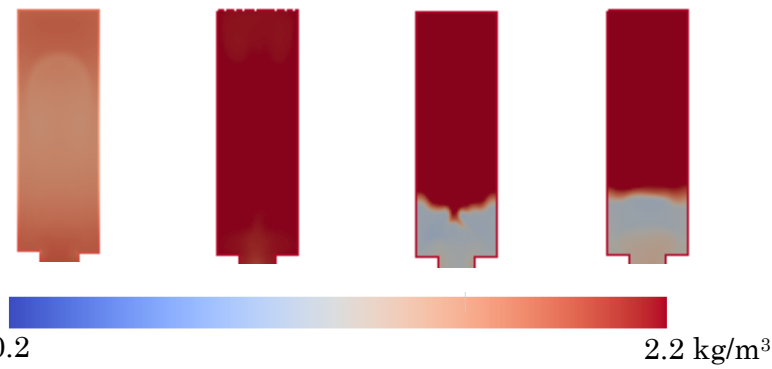


Figure 8 Time history of Density in case of 14mm diameter of orifice

Figures 9 and 10 represent the pressure history at each orifice diameter, in DC and RC. As shown in Fig.7, pressure measurement points in DC and RC are at the central portion of the right side wall. It is found that there is no little difference in the maximum pressure 5mm orifice case, where jet ignition occurs, and 14mm where jet ignition does not occur. But the shape of pressure history is different between two cases. However the shape of the pressure history is smooth on the whole in Fig.9. In contrast, the graph pressure oscillation in Fig.10. It is estimated that in 5mm orifice case compression wave is not nearly affected by ignition, but in 14mm orifice case compression wave is quite affected by ignition. There is the irregular flow near the orifice by reciprocating compression wave in 14mm orifice case, while in 5mm case compression wave is not nearly affected, because there is a regular flow near the orifice at 5mm orifice case. Therefore, jet ignition occurs in 5mm orifice case.

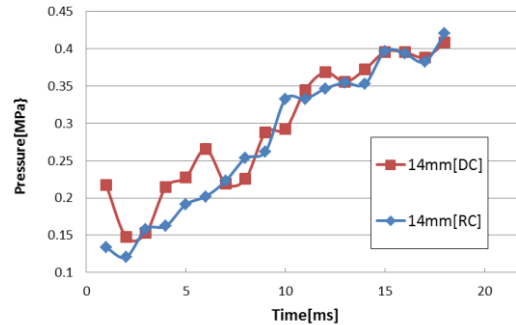
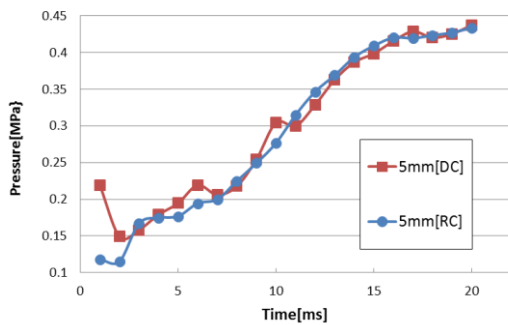


Figure 9 Time history of Pressure in case of 5mm Figure 10 Time history of Pressure in case of 14mm

5. Conclusion

- The types of ignition in RC depends on the orifice diameter
- There is a difference in the fluctuation of the pressure history depending on whether jet ignition occurs or not
- Changing orifice diameter, the shapes of flame before through the orifice are different, This is caused by the difference from the shapes of the flame in MC

Reference

- [1] Gussak LA. High Chemical Activity of Incomplete Combustion Products and a Method of Driver Chamber Torch Ignition for Avalanche of Combustion in Internal Combustion Engines. SAE Transactions: 1976
- [2] Gussak LA. The Role of Chemical Activity and Turbulence Intensity in Pre – Chamber – Torch Organization of Combustion of a Stationary Flow of a fuel – Air Mixture.
- [3] Oppenheim AK. Quest for Controlled Combustion Engines. SAE Transactions, The Journal of Engines: 1998
- [4] Oppenheim, A.K., Beltramo, J., Faris, D.W., Maxson, J.A., Hom, K., Stewart, H.E. Combustion by Pulsed Jet Plumes – Key to Controlled Combustion Engines. SAE Transactions, The Journal of Engine: 1989
- [5] Hensinger, D.M., Maxson, J.A., Hom, K., Oppenheim, A.K. Jet Plume Injection and Combustion. SAE 920414, SAE Transactions: 1992.
- [6] Hayashi, AK., Matsuura, K., Baba, s., Performance of a Flame Jet Ignition System in a Two – Stroke Engine, SAE 2000 World Congress, Society of Auto motive Engineers, 2000
- [7] Suetake, M.,Uchida, N., Hayashi, A.K. Experimental and Numerical Analysis of Jet Ignition. The Proceedings of 17th ICDERS: 1999
- [8] Asami, K., Sakamoto, K., Hayashi, A.K. LIF Measurements of Jet Ignition in Premixed Hydrogen/Air Mixture. Proc. of 7th JSME General Meeting: 2001.
- [9] [http://www.metacomDCom\(Metacomp Technologies Inc. :Website\)](http://www.metacomDCom(Metacomp Technologies Inc. :Website))
- [10] D. Bouris, G. Bergeles. 2D LES of vortex shedding from a square cylinder. Journal of Wind Engineering and Industrial Aerodynamics: 1999
- [11] J.P.Drummond, R.C.Rogers and M.Y.Hussaini. A Numerical Model for Supersonic Reacting Mixing Layers. Computer Methods in Applied Mechanics and Engineering. : 1987
- [12] Jordan M, Eder A, Edlinger B, Mayinger F. Turbulent Quenching and Acceleration of Flames by Highly Blocking Obstacles. FISA Symposium: 1999.
- [13] Mittint, D.N.R. Dabora, E.K. Flame Jet Ignition of Lean Fuel-Air Mixtures. Dynamics of Reactive Systems,vol 105
- [14] A. V. Bjeketvedt, D. Vaagsaether, Experiments with Flame Propagation in a Channel with a Single Obstacle and Premixed Stoichiometric H₂-Air. Gaathaug. K. Combustion Science and Technology : 2010
- [15] Eder, A., Gerlach, C., Mayinger, F. Experimental Observation of Fast Deflagration and Transition to Detonations in Hydrogen-Air-Mixtures.